

Avalanche dynamics, surface roughening and self-organized criticality - experiments on a 3 dimensional pile of rice.

C. M. Aegerter, R. Günther, and R. J. Wijngaarden

Division of Physics and Astronomy, Faculty of Sciences, Vrije Universiteit, De Boelelaan 1081, 1081HV Amsterdam, The Netherlands

(November 15, 2018)

We present a two-dimensional system which exhibits features of self-organized criticality. The avalanches which occur on the surface of a pile of rice are found to exhibit finite size scaling in their probability distribution. The critical exponents are $\tau = 1.21(2)$ for the avalanche size distribution and $D = 1.99(2)$ for the cut-off size. Furthermore the geometry of the avalanches is studied leading to a fractal dimension of the active sites of $d_B = 1.58(2)$. Using a set of scaling relations, we can calculate the roughness exponent $\alpha = D - d_B = 0.41(3)$ and the dynamic exponent $z = D(2 - \tau) = 1.56(8)$. This result is compared with that obtained from a power spectrum analysis of the surface roughness, which yields $\alpha = 0.42(3)$ and $z = 1.5(1)$ in excellent agreement with those obtained from the scaling relations.

DRAFT VERSION: NOT FOR DISTRIBUTION

I. INTRODUCTION

The concept of self-organized criticality (SOC)¹ presents a simple way of modelling slowly-driven out of equilibrium systems. The interesting natural systems thought to exhibit SOC, such as rain-fall², earthquakes³, economic markets⁴, biological evolution⁵, or the brain⁶, are difficult to study in a controlled experiment, and more simple systems have to be found with which the predictions of SOC can be tested quantitatively. Among the first toy systems studied, were sand-piles, however it has been shown that due to the appearance of e.g. kinetic effects, real sand does not behave as an SOC system⁷. Another system, that has shown indications of SOC in a controlled environment is the dynamics of vortices in type-II superconductors. Here, power-law scaling has been observed in the past⁸, however not all authors have found avalanche scaling⁹. This is probably due to the fact that internal avalanches are not measured in the usual setup¹⁰. Recently Behnia *et al.*¹¹ have measured internal avalanches using arrays of Hall-probes, where they do indeed find power-law behavior of the avalanches. The ultimate hall-mark of SOC, however, is the observation of finite size-scaling, indicating a true critical dynamics. So far, there are only two experimental systems, a one dimensional (1d) pile of rice¹² or a 1d pile of steel balls with a random arrangement at its bottom layer¹³, which have been shown to exhibit finite size scaling in their avalanche distributions.

The critical exponents obtained from a finite size scaling analysis, would yield more information on a SOC system, as was discussed by Paczuski *et al.*¹⁴ for models in a stationary critical state. A system evolving through avalanches, which are distributed according to a power-law, will also show roughening dynamics of its surface. This can be seen as an indication to the origin of the abundance of fractal or self-affine structures in nature. Roughening dynamics has been studied extensively in the past, including the study of interfaces in porous media¹⁵, the growth of bacterial colonies¹⁶, the slow combustion¹⁷

or the rupture¹⁸ of paper. These systems are well characterized experimentally and in many cases, the interface dynamics can be modelled analytically by the Kardar-Parisi-Zhang (KPZ) equation¹⁹. In one spatial dimension, the KPZ equation is solved exactly for the case of white noise, such that good comparison between experiment and theory is possible. However, e.g. in the burning of paper, there are avalanches observed in the propagation of the front, which are reminiscent of SOC dynamics²⁰. This has recently been addressed by Alava *et al.*²¹, who proposed a mapping between SOC models and the KPZ equation similar to that of Paczuski and Boettcher²². With this mapping, they have been able to obtain SOC from the KPZ equation, with the proper kind of noise²¹.

Moreover, roughening processes have also been found in the experimental SOC systems discussed above. The profile of a 1d rice pile is a rough interface²³, as is the front of magnetic flux penetrating a thin film superconducting sample²⁴. However, the universal scaling relations derived by Paczuski *et al.*¹⁴ have not yet been tested experimentally. But the fact that both roughening phenomena and avalanche dynamics can be observed in the same experimental system, such as a 3d rice-pile, means that the universal connections between SOC and surface roughening can be tested experimentally.

Here we present a two-dimensional (2d) system, the surface of a 3d pile of rice, showing both roughening behavior and avalanche dynamics. The avalanche dynamics is studied in terms of the avalanche size distribution for different sizes of the field of view, L . This allows the observation of finite size scaling and the determination of the critical exponents D , describing the dependence of the cutoff scale on L , and τ , the exponent of the avalanche size distribution. The roughening behavior is studied via the power spectrum of the surface²⁵, in both space and time, resulting in a determination of the roughness and growth exponents respectively²⁶. The connection between these two phenomena is shown from the derivation of scaling relations between the different

exponents, where we obtain excellent agreement using the experimentally determined values.

The experimental setup for the growth of the rice-pile, as well as the reconstruction method used to determine the structure of the pile and the size of the avalanches is discussed in section II. The avalanche size distributions, and their finite size scaling is presented in section IIIA, together with the determination of the critical exponents. In section IIIB, the surface roughness is analyzed and the necessary techniques are briefly introduced. Still in section IIIB, the scaling relations between the roughness exponents and the critical exponents are introduced. These results are also put into a wider context and compared with results from KPZ roughening systems²⁷.

II. EXPERIMENTAL DETAILS

The experiments were carried out on long grained rice with dimensions of typically $\sim 2 \times 2 \times 7 \text{ mm}^3$, similar to rice A of ref.¹². The pile was grown from a uniform line source 1 m wide. This uniform distribution was achieved via a custom built mechanical distributor based on a nail-board producing a binary distribution²⁸. The actual setup consists of a board with an arrangement of triangles as shown in Fig. 1. This means that the possible pathways of the rice are continuously split at each level, such that at the bottom we end up with a row of 64 uniformly distributed compartments. The uniformity of the distribution was measured to be of the order of 5%.

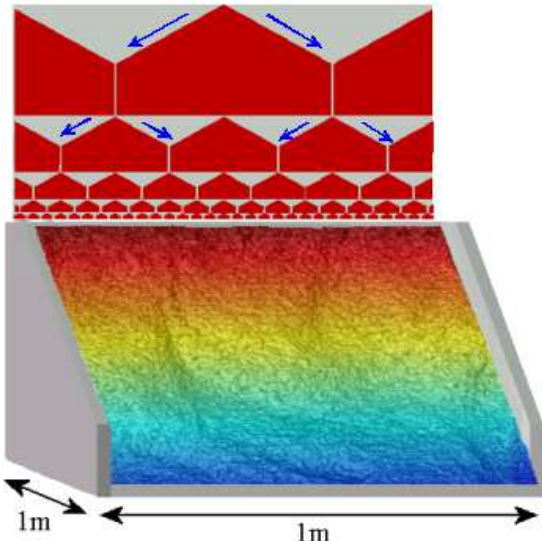


FIG. 1. A schematic image of the setup. The distribution board can be seen on top, where rice is dropped from a single point and subsequently divided into even compartments. Within the wooden box bounding the rice pile, a reconstruction of its surface is shown, as it is used in the further analysis.

At the bottom of the distributor, the grains are slowed down by a sheet of plastic before they hit the top of the pile. The rice is fed to the top of the distribution board, from a point source, which drops rice at an average rate of $\sim 5 \text{ g/s}$. This corresponds to 1500 grains per image,

which means that over the length of the line there are 1 to 2 grains dropped per place. This rate is uniform over the time scale between two images.

Once a rice pile is grown, we measure the further evolution of the surface coordinates using a specially developed real-time technique based on the projection of a set of lines. In order to increase the spatial resolution in the direction of growth, we use a set of lines in the base colors (red, green and blue), which can be easily separated digitally for the analysis. The lines are projected at a right angle to the average surface of the pile and observed at 45° to both the direction of projection as well as the surface. This is illustrated in Fig. 2, where a raw image is shown together with the lines extracted from it. From the distortions of the lines observed in this way, the coordinates in 3d space of the pile surface can be calculated by simple geometry²⁸. With this reconstruction technique, the 3d coordinates of the whole field of view can be determined with an accuracy of 2-3 mm, as we have checked on a number of test surfaces. Using both structured and smooth surfaces, the resolution and accuracy were determined independently. Since the resolution is roughly matched with the size of the grains, the method is well suited for the present purpose.

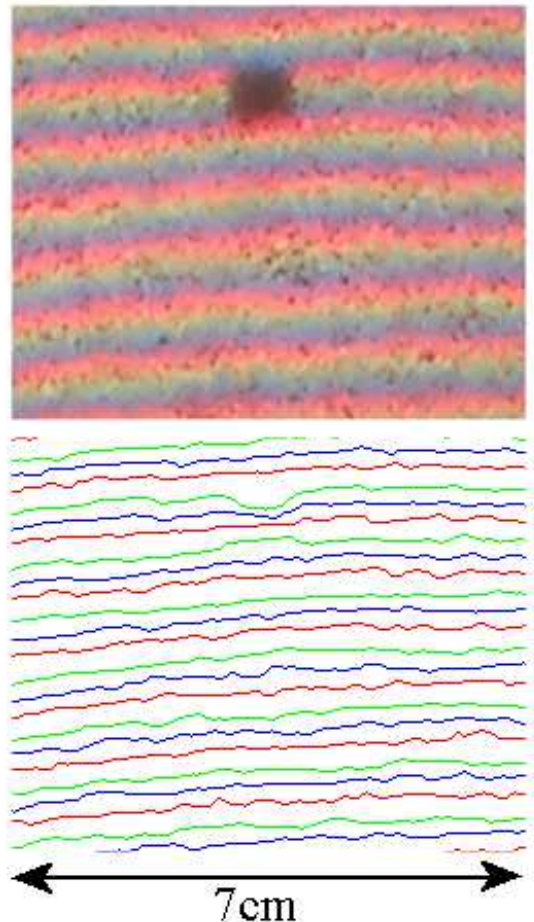


FIG. 2. A raw image of the rice pile with the identified lines. From the distortions of the lines, the surface geometry is obtained. The dark spot in the image indicates a reference point.

In a single experimental run, the growth is studied for a period of ~ 4 hours, with a picture taken every 30 s. Thus an experiment consists of ~ 480 images. The pictures are taken with a high resolution digital camera, having a resolution of 2048×1536 pixels. For every time step, the surface structure is reconstructed, which gives information about the roughening process, as well as the avalanche dynamics.

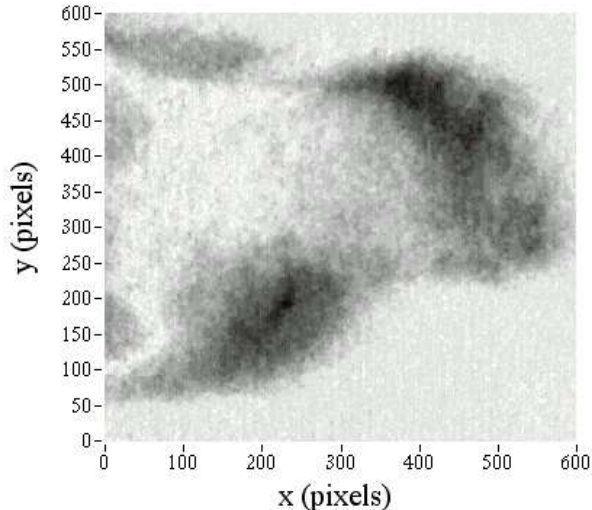


FIG. 3. A snapshot of an avalanche, given by the height difference of two subsequent images. In the picture, the height is given by the grey-scale with white corresponding to $\Delta h = 0$ and black to $\Delta h = 15$ mm. Integrating the height difference $\Delta h(x, y)$ over the area gives the size of the avalanche in terms of a volume, or in terms of the number of moved grains from the volume occupied by a grain $V_{grain} = 35$ mm³.

The size and shape of the avalanches can be determined from the height difference of the surface between two consecutive images. The overall growth of the pile is subtracted from this difference, however this correction is negligible and does not influence the results. This is shown in Fig.3, where the height difference $\Delta h(x, y)$ is shown for a medium size avalanche. This allows the study of internal avalanches instead of just the off-edge ones, which has proven to be important in previous studies (for instance on superconducting vortex avalanches¹¹ and 1d piles of rice¹²). In order to obtain the size of such an avalanche, $|\Delta h|$ is integrated over the area, which yields the displaced volume, ΔV , corresponding to the size of the avalanche in mm³. In order to use natural units, we will in the following measure the size of the avalanche in terms of the number of toppled grains, which is $s = \Delta V / V_{grain}$, where $V_{grain} \simeq 35$ mm³ is the volume of a single grain of rice.

The data discussed in this article was obtained in three separate experiments, with a total of 1330 images.

III. RESULTS

In this section the experimental results are presented. We first show that there is finite size scaling in the

avalanche statistics, which indicates the appearance of a critical state in the system. Second, we characterize the surface roughness of the rice pile in 2d, both in space and time. The two characteristic exponents, α for the spatial behavior, and z for the dynamics²⁶ can also be obtained from scaling relations of the critical exponents of the avalanche statistics and are in excellent agreement with those determined from a standard power-spectrum analysis.

A. Avalanche Dynamics

The time dependence of the displaced volume, ΔV , in each time step is shown in Fig. 4, for all three experiments discussed here. In the figure, the data are shown for avalanche sizes integrated over the total field of view of 600×600 mm².

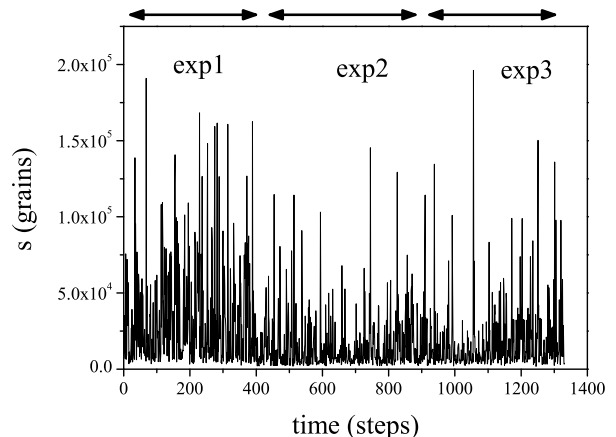


FIG. 4. The time evolution of the integrated height difference for the three experimental runs studied. As can be seen, times of relative rest are punctuated by large avalanches, which appear intermittently. When studying the distribution of avalanche sizes (see Fig. 5), it is found that there is no intrinsic size to the avalanches, but that they are distributed according to a power-law. The different experimental runs are indicated by arrows.

A histogram of these data, giving the avalanche size distribution is shown by the diamonds in Fig. 5a). In that figure, size distributions of subsets of the data corresponding to smaller fields of view ($L = 50, 150$ and 300 mm) are also shown. Due to experimental resolution, the smallest avalanches measured for each subset depend on the size of that subset. The range of sizes from 50×50 mm² to 600×600 mm² spans more than a decade and all of the data taken together show a power-law scaling of the size distribution over three decades, with an exponent of $\tau = 1.20(5)$.

These data can however be scaled to fall onto a single curve, as shown in Fig 5b). Here the avalanche sizes are scaled with L^{-D} and the probabilities are scaled with s^τ . The good curve collapse visible in Fig 5b) indicates the presence of finite size scaling in the data, one of the hallmarks of critical behavior in a system and thus evidence

of the appearance of SOC in the 3d rice pile.

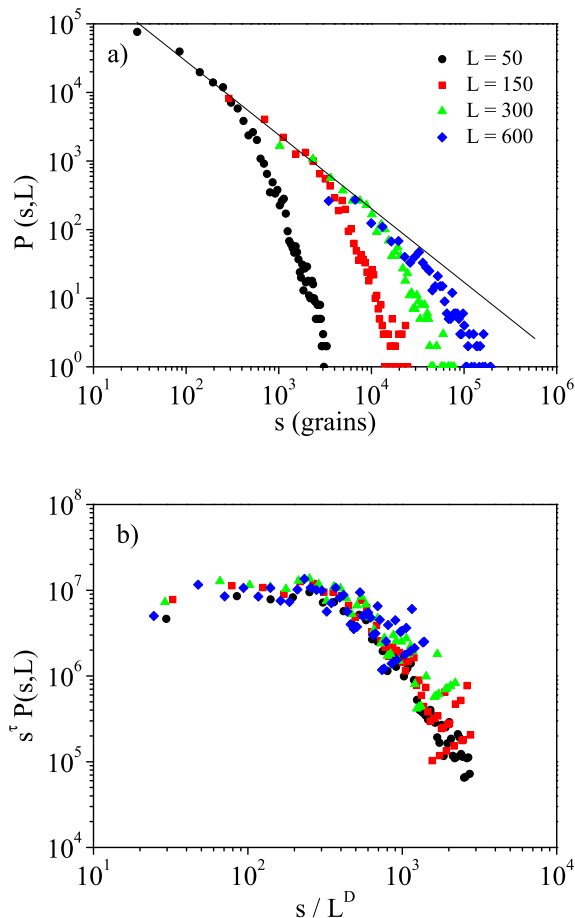


FIG. 5. a) The unscaled size distribution functions for the avalanches from different subsets of the experiments corresponding to sizes of $L = 50, 150, 300$ and 600 mm. Given the asymptotic dependence of all them together, there is power-law behavior over at least three decades, with an exponent of $\tau = 1.20(5)$. b) The same data, scaled to produce a curve collapse. The sizes of the avalanches are scaled with L^{-D} and the probabilities are scaled with s^τ . The values used to obtain the best curve collapse are $\tau = 1.21(2)$ and $D = 1.99(2)$.

Due to the finite size scaling found from the curve collapse, the avalanche size distribution as a function of system size can be written as a function of one parameter only:

$$P(s, L) = s^{-\tau} f\left(\frac{s}{L^D}\right), \quad (1)$$

where $f(x)$ is constant up to a cutoff scale

$$s_{co} \propto L^D. \quad (2)$$

The exponents τ and D used to obtain the curve collapse in Fig. 5b) were $\tau = 1.21(2)$ and $D = 1.99(2)$. We note here that in usual finite size scaling, separate experiments are used instead of subsets. However, as we have tested on simulations of a 2d version of the Oslo-model²⁹, finite size scaling using subsets yields the same exponents, but

is much more easily implemented experimentally. As an additional test, the avalanche dimension can be determined directly using a box-counting method in 3d. This yields $D = 2.05(10)$ consistent with the result from finite size scaling.

B. Surface Roughening

The roughness of a surface can be characterized in different ways. Most commonly, this is done via the width of the interface as given by its standard deviation²⁶. For a 2d surface, this is given by

$$w^2(L) = \frac{1}{L^2} \sum_{i,j=1}^L (h(i,j) - \langle h \rangle)^2, \quad (3)$$

where $\langle h \rangle$ is the average profile of the surface height. When the roughness of the surface has reached saturation, its value w_{sat} , will scale with the system size as a power-law, $w_{sat} \propto L^\alpha$, where α is the roughness exponent.

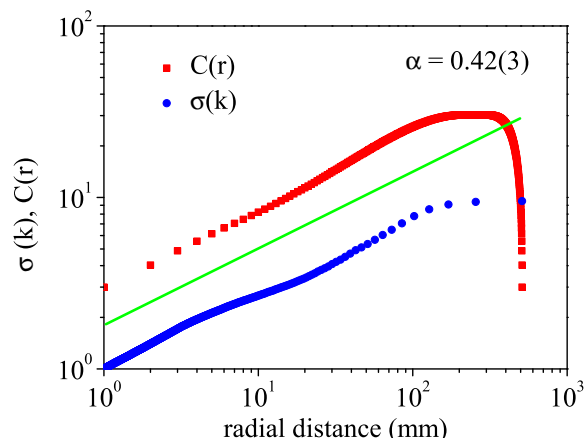


FIG. 6. Determination of the roughness exponent from a power-spectrum analysis as well as from the correlation function $C(x)$ (squares). After subtracting the average slope of the pile, its 2d power spectrum is calculated. After taking a radial average, it is integrated over k -space in order to give the distribution function σ , which follows a power-law dependence $\sigma \propto k^{-\alpha}$, with a roughness exponent $\alpha = 0.42(3)$. Similarly, the correlation function $C(x) \propto x^\alpha$ (squares) is calculated from the pile surface, resulting in the same exponent as that determined from the distribution function.

A similar type of analysis can be achieved via the power spectrum of the surface. Here, one has the advantage that better statistics can be obtained, since the whole surface can be used at once²⁵. We determined the power spectrum from a radial average of the 2d Fourier transform of the surface

$$S(k) = |\hat{h}(k_x, k_y)|^2, \quad (4)$$

where $k = (k_x + k_y)^{1/2}$. The Fourier transforms were performed via an FFT algorithm, which is why a data

subset corresponding to a power of two (512x512) was used. From the power spectrum we then determine the distribution function $\sigma(k)$

$$\sigma^2(k) = \int_0^k S(\kappa)\kappa d\kappa, \quad (5)$$

from which it can be shown²⁵ that $\sigma(2\pi/k) = w(\ell)$, where $\ell = 2\pi/k$ is the length scale over which the width is calculated. The roughness exponent α can therefore be reliably obtained from a determination of $\sigma(k)$. An alternative way of obtaining the roughness exponent is via the two point correlation function²⁶.

$$C(\vec{x}, t) = \left(\langle (h(\vec{\xi}, \tau) - h(\vec{x} + \vec{\xi}, t + \tau))^2 \rangle_{\vec{\xi}, \tau} \right)^{1/2}, \quad (6)$$

the radial average of which obeys the same scaling behavior as the distribution function²⁶.

In Fig. 6, the correlation and distribution functions for the rice-pile surface is shown, averaged over all time steps of all experiments (1330 images). The part of the surface studied consists of 512x512 mm in the center of the surface laterally (along the horizontal direction) and starting from a height of 200 mm. As can be seen from the double logarithmic plot, there is power-law scaling with an exponent, $\alpha = 0.42(3)$.

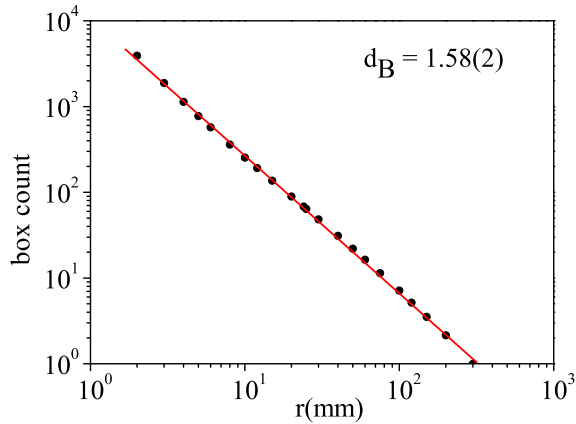


FIG. 7. Determination of the fractal dimension of the avalanches. Over all experiments, avalanches with a size two standard deviations bigger than the average were studied. The contours are derived from a thresholding at the value of the mean height difference for each image. The fractal dimension is subsequently determined from a simple box counting method.

The scaling behavior of the interface width can, however, also be determined from the cut-off size of the avalanches in a system with size L . The size of such an avalanche will be proportional to the maximal height difference, given by the saturation width w_{sat} , times the maximal area of the avalanche. As can be seen from Fig. 3, the avalanche-shape is a fractal, which means that $s_{co} \propto w_{sat} L^{d_B}$, where d_B is the fractal dimension of the cluster of displaced grains. Equating this expression with Eq. 2, one obtains $w_{sat} \propto L^{D-d_B}$, which implies the scaling relation

$$\alpha = D - d_B. \quad (7)$$

Such a scaling relation between the roughness exponent and the exponents characterizing the avalanches was also derived by Paczuski *et al.*¹⁴ from different arguments.

In order to determine d_B in an accurate manner, we studied avalanches more than two standard deviations bigger than the average size. This corresponds to a subset of ~ 100 images from all experiments. After thresholding the height difference fields $\Delta h(x, y)$ at their mean value, we applied a simple box counting method³⁰ to the resulting clusters. This is shown in Fig. 7, where the number active pixels in a box of given size is shown as a function of the box size. The result is a power law with an exponent of $-1.58(2)$, indicating a fractal dimension of $d_B = 1.58(2)$. Inserting this value into scaling relation (7), the roughness exponent is found to be $\alpha = 0.41(3)$, in excellent agreement with that determined from the roughness analysis.

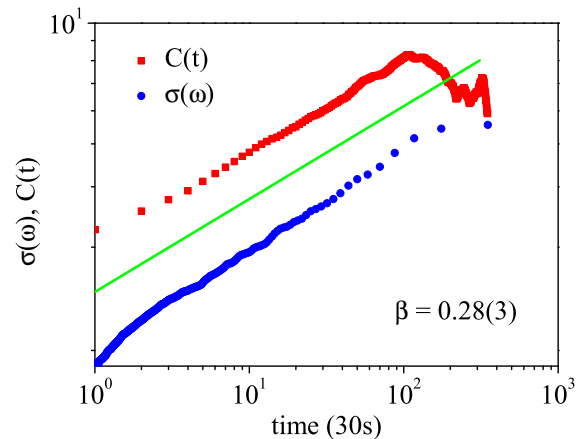


FIG. 8. Determination of the growth exponent from a power-spectrum analysis. Here, the distribution function σ has been determined from the time dependence of the height of each pixel. The data show a power-law dependence $\sigma \propto \omega^{-\beta}$, with a growth exponent $\beta = 0.28(3)$. The same result is obtained via the correlation function, indicated by the open symbols. From the growth and roughness exponents, the dynamic exponent $z = \alpha/\beta = 1.5(1)$ can be determined.

The dynamics of the roughening process is likewise analyzed via the distribution function. In contrast to the roughness analysis above, we now determine the distribution function for the time dependence $h_{i,j}(t) - \langle h_{i,j} \rangle_t$ for each pixel, where $\langle \cdot \rangle_t$ denotes the average over the duration of the experiment. Again, the distribution function, given by

$$\sigma^2(\omega) = \int |\hat{h}(\omega)|^2 d\omega, \quad (8)$$

is equal to the momentary width, $\sigma(2\pi/\omega) = w(t)$. Thus the growth exponent β , describing the scaling of the width with time, can be determined from the distribution function. Again, the correlation function shows the

same scaling behavior in time, allowing a separate determination of β . Both results are shown in Fig. 8, where it can be seen that there is good power-law scaling of the distribution function, as well as the correlation function, over two decades with an exponent of $\beta = 0.28(3)$. Another way of describing the dynamics of an interface is via the dynamic exponent z , which describes the scaling of the saturation time with the system size

$$t_{\times} \propto L^z. \quad (9)$$

It can be easily obtained²⁶ from the roughness and growth exponents via

$$z = \frac{\alpha}{\beta}. \quad (10)$$

From the values determined above we thus obtain $z = 1.5(1)$.

The dynamic exponent, z , can also be derived from a scaling relation using the critical exponents of the avalanche dynamics. The saturation time, t_{\times} , will be roughly given by the time it takes for an avalanche of the cut-off size, s_{co} , to appear. Since material is added to the system at a constant rate, the number of grains added until a cut-off avalanche occurs is proportional to the cross-over time t_{\times} . On the other hand, the material added not only result in an avalanche of size s_{co} , but will also be lost by smaller avalanches, such that the total material necessary to obtain an avalanche of size s_{co} can be estimated from:

$$\int_0^{s_{co}} sP(s)ds \propto s_{co}^{2-\tau}. \quad (11)$$

From Eq. 2, we obtain for the cross-over time $t_{\times} \propto L^{D(2-\tau)}$. With Eq. 9, this immediately leads to the scaling relation

$$z = D(2 - \tau), \quad (12)$$

which was also derived by Paczuski *et al.*¹⁴ from more general arguments. Using the values for D and τ determined above from the curve collapse of the avalanche size distributions, we obtain $z = 1.56(8)$, which is again in very good agreement with the result of the power spectrum analysis, $z = 1.5(1)$. Note also that the exponents α and z fulfill the KPZ scaling relation¹⁹ $\alpha + z = 2$, which is valid independent of the dimension of the system and depends only on the fact that the growth is driven by height gradients. Furthermore, the roughness exponent $\alpha = 0.42(3)$ is in good agreement with a numerical determination of the behavior of the 2d KPZ equation²⁷. The connection between roughening and SOC will be discussed in more detail below.

IV. CONCLUSIONS

In conclusion, we have presented results on both the avalanche and the roughening behavior of an experimental SOC system. In addition, we presented simple arguments for universal scaling relations, derived by Paczuski

*et al.*¹⁴ on general grounds, connecting the avalanche and roughening behavior. We obtain *quantitative* agreement of the experimental exponents characterizing the roughness and those describing the avalanche statistics. This means that the roughening of the surface of the pile is governed by its underlying avalanche dynamics, which was already conjectured from models of interface depinning. Earlier experimental studies^{12,23} have considered the avalanche dynamics and the roughening behavior of the 1d version of the present system, where finite size scaling was also found¹². The above scaling relations, showing quantitatively the connection between the two phenomena were not previously tested.

The fact that KPZ dynamics is observed in a SOC system, as indicated by the fact that the roughness and dynamic exponents obtained here fulfill the KPZ scaling relation, is surprising. This is mostly because in SOC systems, the critical state is self organized, whereas in KPZ systems, the roughening is put into the dynamics by obeying the proper symmetries. However, it has been argued by Alava *et al.*²¹, that there is a mapping of SOC models, which naturally lead to the necessary symmetries. In this context, it should also be noted that experiments on KPZ systems such as burning paper have also observed 'avalanches' in the advance of fronts²⁰.

V. ACKNOWLEDGEMENTS

This work was supported by FOM (Stichting voor Fundamenteel Onderzoek der Materie), which is financially supported by NWO (Nederlandse Organisatie voor Wetenschappelijk Onderzoek).

¹ P. Bak, C. Tang, and K. Wiesenfeld, Phys. Rev. Lett. **59**, 381 (1987) and Phys. Rev. A **38**, 364 (1988).

² O. Peters, C. Hertlein, and K. Christensen, Phys. Rev. Lett. **88**, 018701 (2002); O. Peters, and K. Christensen, preprint.

³ see e.g. P. Bak, K. Christensen, L. Danon, and T. Scanlon, Phys. Rev. Lett. **88**, 178501 (2002); A. Sornette, and D. Sornette, Europhys. Lett. **9**, 197 (1989); J. M. Carlson, J. S. Langer, and B. E. Shaw, Rev. Mod. Phys. **66**, 657 (1994).

⁴ see e.g. J. A. Scheinmann, and M. Woodford, Am. J. Econ. **84**, 417 (1994); P. Bak, K. Chen, J. A. Scheinmann, and M. Woodford, Ricerche Economiche **47**, 3 (1993).

⁵ see e.g. J. Bascompte, and R. V. Solé, Trends Ecol. Evol. **10**, 361 (1995); H. Flyvbjerg, P. Bak, and K. Sneppen, Phys. Rev. Lett. **71**, 4087 (1993); S. A. Kaufmann, and S. J. Johnsen, J. Theor. Biol. **149**, 467 (1991).

⁶ D. Stassinopoulos, and P. Bak, Phys. Rev. E **51**, 5033 (1995).

⁷ H. M. Jaeger, S. R. Nagel, and R. P. Behringer, Rev. Mod. Phys. **68**, 1259 (1996); S. R. Nagel, *ibid.* **64**, 321 (1992) and references therein.

- ⁸ S. Field, J. Witt, and F. Nori, Phys. Rev. Lett. **74**, 1206 (1995); C. M. Aegerter, Phys. Rev. E **58**, 1438 (1998).
- ⁹ see e.g. R. J. Zieve, T. F. Rosenbaum, H. M. Jaeger, G. T. Seidler, G. W. Crabtree, and U. Welp, Phys. Rev. B **53**, 11849 (1996); E. R. Nowak, O. W. Taylor, L. Liu, H. M. Jaeger, and T. I. Selinder, Phys. Rev. B **55**, 11702 (1997).
- ¹⁰ J. Feder, *Fractals* (Plenum, New York, 1989).
- ¹¹ K. Behnia, C. Capan, D. Mailly, and B. Etienne, Phys. Rev. B **61**, R3815 (2000); K. Behnia, C. Capan, D. Mailly, and B. Etienne, J. Mag. Mag. Mat. **226**, 370 (2001).
- ¹² V. Frette, K. Christensen, A. Málthe-Sørenssen, J. Feder, T. Jøssang, and P. Meakin, Nature (London) **379**, 49 (1996).
- ¹³ E. Altshuler, O. Ramos, C. Martinez, L. E. Flores, and C. Noda, Phys. Rev. Lett. **86**, 5490 (2001).
- ¹⁴ M. Paczuski, S. Maslov, and P. Bak, Phys. Rev. E **53**, 414 (1996).
- ¹⁵ M. A. Rubio, C. A. Edwards, A. Dougherty, and J. P. Gollub, Phys. Rev. Lett. **63**, 1685 (1989); V. K. Horváth, F. Family, and T. Vicsek, J. Phys. A **24**, L25 (1991); S. He, G. L. M. K. S. Kahanda, and P.-Z. Wong, Phys. Rev. Lett. **69**, 3731 (1992).
- ¹⁶ E. Ben-Jacob, O. Shochet, A. Tenenbaum, I. Cohen, A. Czirók, and T. Vicsek, Nature(London) **368**, 46 (1994); S. Matsuura, and S. Miyazima, Fractals **1**, 336 (1993); T. Vicsek, M. Cserző, and V. K. Horváth, Physica A **167**, 315 (1990).
- ¹⁷ J. Maunuksela, M. Myllys, O. P. Kähkönen, J. Timonen, N. Provatas, M. J. Alava, and T. Ala-Nissila, Phys. Rev. Lett. **79**, 1515 (1997).
- ¹⁸ J. Kertész, V. K. Horváth, and F. Weber, Fractals **1**, 67 (1993).
- ¹⁹ M. Kardar, G. Parisi, and Y.-C. Zhang, Phys. Rev. Lett. **56**, 889 (1986).
- ²⁰ A. Myllys, J. Maunuksela, A. Alava, T. Ala-Nissila, J. Merikoski, and J. Timonen, Phys. Rev. E **64**, 036101 (2001); and J. Timonen, private communication.
- ²¹ M. Alava, and K. B. Lauritsen, Europhys. Lett. **53**, 569 (2001); G. Szabo, M. Alava, and J. Kertesz, Europhys. Lett. **57**, 665 (2002); M. Alava, J. Phys. C **14(9)**, 2353 (2002).
- ²² M. Paczuski, and S. Boettcher, Phys. Rev. Lett. **77**, 111 (1996).
- ²³ A. Málthe-Sørenssen, J. Feder, K. Christensen, V. Frette, and T. Jøssang, Phys. Rev. Lett. **83**, 764 (1999).
- ²⁴ R. Surdeanu, R. J. Wijngaarden, E. Visser, J. M. Huijbregtse, J. H. Rector, B. Dam, and R. Griessen, Phys. Rev. Lett. **83**, 2054 (1999).
- ²⁵ J. Schmittbuhl, J.-P. Vilotte, and S. Roux, Phys. Rev. E **51**, 131 (1995); M. Siegert *ibid.* **53**, 3209 (1996); J. M. Lopez, M. A. Rodriguez, and R. Cuerno, *ibid.* **56**, 3993 (1997).
- ²⁶ A. L. Barabasi and H. E. Stanley *Fractal Concepts in Surface Growth* (Cambridge University Press, 1995).
- ²⁷ J. G. Amar, and F. Family, Phys. Rev. A **41**, 3399 (1990).
- ²⁸ R. Günther, Masters Thesis, Vrije Universiteit (2002).
- ²⁹ C. M. Aegerter, Physica A **319**, 1 (2003).
- ³⁰ B. B. Mandelbrot, *The fractal geometry of nature* (Freeman, New York, 1983).